Short Crack Growth Behavior and Its Relation to Notch Sensitivity and VHCF

Y. Kondo[1,a], M. Endo[2,b] and A. J. McEvily[3,c]

[1]Dept. of Mech. Engng, Kyushu Univ., 744 Moto-oka, Nishi-ku, Fukuoka 811-0395, Japan

[2]Dept. of Mech. Engng, Fukuoka Univ., 8-19-1 Nanakuma, Jonan-ku, Fukuoka814-0180, Japan

[3]Inst. Mats. Science, Univ. of Connecticut, 97 North Eagle Road, Storrs, CT 0629-3136, U.S.A.

[a]ykondo@mech.kyushu-u.ac.jpl, [b]endo@fukuoka-u.ac.jp, [c]mcevily@mail.ims.uconn.edu

Keywords: Short fatigue cracks, Fatigue notch sensitivity, Very high cycle fatigue, Fatigue crack closure, Elastic-plastic fatigue, Kitagawa effect.

Abstract. In a series of experiments, short fatigue cracks of an initial length of from 10 to several hundred microns in length, were grown in bending in a steel under constant amplitude loading conditions, and the rate of fatigue crack growth was determined. A modified LEFM analysis based upon the relation $da/dN = A(\Delta K_{eff} - \Delta K_{effth})^2$ was used to predict the threshold level of these cracks. The results of the analysis compared favorably with the experimental results. It is shown that the growth behavior of short fatigue cracks is also related to fatigue notch sensitivity and to the very high cycle fatigue (VHCF) behavior of Ti-6Al-4V.

Introduction

The growth of short fatigue cracks to failure can take up most of the fatigue lifetime, and it is therefore important to be able to analyze their behavior. A procedure for doing so is presented in this paper. It will also be shown that a knowledge the characteristics of short fatigue crack growth behavior can be helpful in understanding such fatigue phenomena as fatigue notch sensitivity and the very high cycle fatigue (VHCF) behavior of titanium. There are three aspects of short fatigue crack growth which distinguish it from long fatigue crack growth, namely:

1. Elastic-plastic crack growth rather than linear-elastic crack growth because of a high ratio of applied stress to the yield stress,
2. Control of the rate of fatigue crack growth by the stress amplitude rather than the stress intensity factor range for vanishingly small crack lengths, and
3. A transition in crack closure from zero for a newly formed crack up to a level corresponding to that of a long crack as the crack increases in length.

We begin by reviewing the basic equations involved [1,2].

Analysis

The basis equation governing the growth of both long and short cracks is

$$\frac{da}{dN} = \frac{A'}{\sigma_Y E}[\Delta K_{eff} - \Delta K_{effth}]^2 \qquad (1)$$

where a is the crack length, N is the number of cycles, A' is a dimensionless material constant, σ_Y is the yield strength, E is Young's modulus, ΔK_{eff} is the effective range of the stress intensity factor equal to K_{max} - K_{op} where K_{op} corresponds to the crack opening level, and ΔK_{effth} is the range of K_{eff} at the threshold level, which is taken to correspond to growth rate of 10^{-11} m/cycle.

Eq. 1 expresses the rate of fatigue crack growth as a function of the crack tip opening displacement, and is dimensionally correct. The equation is simplified to the form

$$\frac{da}{dN} = A[\Delta K_{eff} - \Delta K_{effth}]^2 \quad (2)$$

where $A = \frac{A'}{\sigma_Y E}$.

If in addition to a cyclic mode of growth a static component is also present as is the case when K_{max} approaches K_c, the fracture toughness, then Eq. 2 can be written as

$$\frac{da}{dN} = A[\Delta K_{eff} - \Delta K_{effth}]^2[1 + \frac{\Delta K_{eff}}{K_c - K_{max}}] \quad (3)$$

An example of the use of Eq. 3 in the long crack range is given in Fig. 1 for Ti-6Al-4V [3]. Note there is transition where the plastic zone size equals the α-grain size.

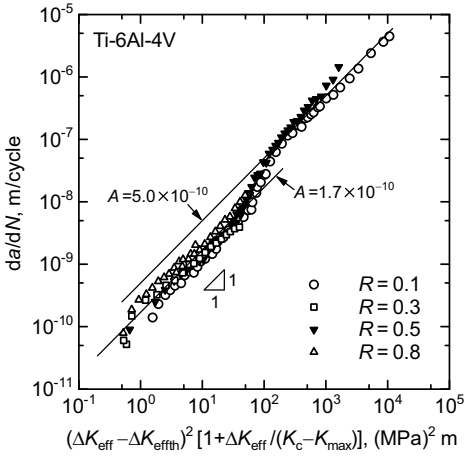

Fig.1. The rate of fatigue crack growth in Ti-6Al-4V as a function of the parameter given in Eq. 3 [3].

In order to deal with short fatigue crack growth, Eq. 3 is modified to take into account the three factors mentioned above. The resultant expression for the rate of fatigue crack growth is

$$\frac{da}{dN} = A([(\sqrt{2\pi r_e F} + Y\sqrt{\pi a F})\Delta\sigma - (1 - e^{-k\lambda})(K_{op\max} - K_{\min}) - \Delta K_{effth}]^2 \quad (4)$$

where r_e is a material length constant of the order of one micron in size and defined by

$$r_e = \left(\frac{\Delta K_{effth}}{2(\sqrt{2} + Y)\sigma_{wo}}\right)^2 \frac{1}{\pi F} \quad (5)$$

where σ_{wo} is the endurance limit under fully reversed loading, Y is a crack shape factor equal to 0.73 for a semi-circular surface crack, and equal to 1.12 for a through-crack in a plate. F is the elastic-plastic correction factor defined by

$$F = (1 + \sec\frac{\pi}{2}\frac{\sigma_{\max}}{\sigma_y}) \quad (6)$$

In Eq. 4, k [m^{-1}] is a material constant which determines the rate of crack closure development, λ is the length of a newly formed crack, and $K_{op\max}$ is the crack opening level for long crack. An example of the use of Eq. 4 will be given in the next section.

Growth of Short Cracks

In this section a comparison of the short-crack experimental results obtained by Kondo et al. [4] will be made with predictions based upon Eq. 4.

Kondo et al. tested in fully reversed bending a 0.26 carbon steel whose yield strength was 305 MPa. The specimen configuration is shown in Fig. 2. A 0.11 mm deep notch was used to localize the cracking process, and pre-cracks crack were grown at R = -2 to desired lengths. Fatigue thresholds were determined for initial crack lengths which included the notch depth ranging from 15 microns to one millimeter. For initial crack lengths, including the depth of notch, less that 0.17 mm, after pre-cracking, material was removed by grinding and polishing. Signals from the strain gauges mounted on the specimens were entered into a computer and an offset-displacement curve was obtained to determine the crack length.

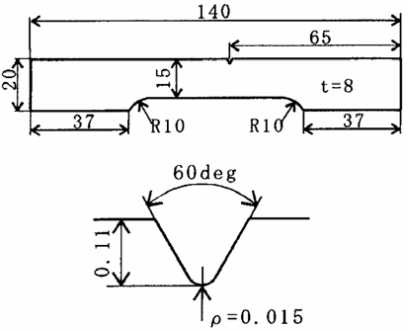

Fig. 2. Specimen configuration

The curves of threshold stress amplitudes calculated based upon Eq. 4 are shown in Fig. 3. The material constants used in the calculations are listed in Table 1.

Material	σ_Y [MPa]	σ_{uts} [MPa]	σ_{w0} [MPa]	k [m^{-1}]	K_{opmax} [MPam$^{-1/2}$]	ΔK_{effth} [MPam$^{-1/2}$]	r_e [μm]
0.26 carbon steel	305	544	240	6000	3.0	3.0	1.34

Table 1. Material constants for 0.26 carbon steel.

For the calculation of r_e, Y was taken to be 0.73. Therefore,

$$r_e = \left(\frac{\Delta K_{effth}}{2(\sqrt{2}+0.73)\sigma_{w0}}\right)^2 \frac{1}{\pi F} = \left(\frac{3}{2(\sqrt{2}+0.73)240}\right)^2 \frac{1}{\pi \times 2.022} = 1.34\times 10^{-6} m \quad (7)$$

For R = -1, K_{min}= - $K_{max,}$ and with the use of Eq.4, σ_a, the fatigue strength for a specimen containing a crack with da/dN set equal to zero ([10^{-11}]m/cycle) can be expressed as a function of crack length as

$$\sigma_a = \frac{(1-e^{-k\lambda})K_{op\max} + \Delta K_{effth}}{(\sqrt{2\pi r_e F} + 1.122\sqrt{\pi a F})(1+e^{-k\lambda})} \quad (8)$$

Note that the determination of σ_a needs iteration since F contains σ_a.

As seen in Fig. 3, as the crack length increases in length from an initial value of 100 μm, the value of the stress amplitude at threshold which initially corresponds to the effective threshold condition, σ_{ai}, increases to a maximum in order to overcome the increase in resistance to crack growth due to the development of crack closure in the wake of the crack. The maximum stress amplitude corresponds to

σ_w, the fatigue strength for the corresponding initial crack size. At stress amplitudes between σ_{ai} and σ_w, non-propagating cracks will form.

If the initial crack length in Fig. 3 is 10 μm, σ_w will be equal to σ_{ai}, because in this range of very short crack lengths the rate of increase in the stress intensity factor, the driving force, is higher than the rate of increase in the resisting force associated with development of crack closure.

Fig. 4 shows the good agreement between the results of calculations based upon Eq. 4 and the experimental results of Kondo et al.

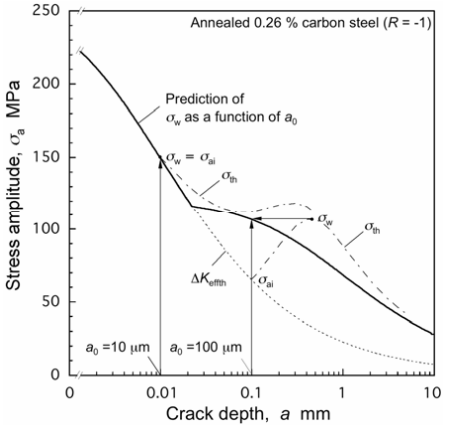

Fig. 3. An example of the use of Eq. 4 in predicting σ_w as a function of a_0 in the short crack range. [13].

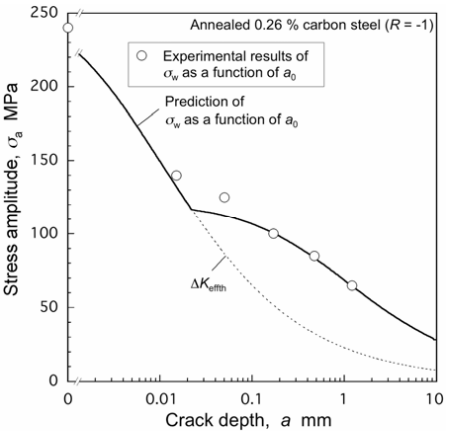

Fig. 4. A comparison of experimental results for σ_w obtained by Kondo et al. [4] with predicted behavior based upon Eq.

Fatigue Notch Sensitivity

When specimens containing notches or holes of known elastic stress concentration factor K_T are tested under cyclic loading and their fatigue strengths noted, two observations are generally made. One is that the stress concentration factor in fatigue, K_F, which is given as the ratio of the unnotched specimen fatigue strength to that of the notched specimen fatigue strength, is generally less than K_T. The other is that the smaller the size of the notch or hole the smaller is the value of K_F. This phenomenon has been dubbed the notch size effect. In order to deal it on the engineering level, various empirical relationships have been advanced, notably those by Kuhn and Hardrath [5], Peterson [6] and the JSME [7]. An important advance in understanding why K_F is less than K_T was made by El Haddad, Topper and Smith [8] based upon the growth behavior of small fatigue cracks. Experimental results obtained by El Haddad, Topper and Smith [8] under R = -1 loading conditions will be used to compare with predictions made on the basis of Eq. 4. El Haddad et al. tested a steel, designated as G40.11. Table 2 lists the material properties of this steel as well as the material constants used in our analysis. The value of K_{opmax} is consistent with the data of El Haddad et al [8]. The value of r_e was obtained by means of Eq. 5.

Material	σ_Y [MPa]	σ_{uts} [MPa]	σ_{w0} [MPa]	k [m^{-1}]	K_{opmax} [$MPam^{-1/2}$]	ΔK_{effth} [$MPam^{-1/2}$]	r_e [μm]
G40.11 Steel	376	676	276	6000	5.5	3.0	1.2

Table 2. Material constants for G40.11 steel

El Haddad et al. tested plate specimens containing holes of either 0.2 mm radius, 0.48 mm radius or 4.8 mm radius, and were interested in the factors that led to the non-propagation of cracks. It is assumed that the specimens were tested with the holes in the as-machined condition and that through-thickness fatigue cracks were created as a result.

In the case of a specimen containing a hole, for fully reversed loading (R = -1), the stress amplitude at the threshold level (da/dN = 0) for a through-thickness crack (2D) emanating from a centrally located circular hole of radius a_0 in a plate can be written as

$$\sigma_{\text{amp}} = \frac{\Delta K_{\text{effth}} + \left(1 - e^{-k\lambda}\right) K_{\text{opmax}}}{Y(\lambda_1)\left[\sqrt{2\pi r_e F} + 1.0\sqrt{\pi\lambda F}\right]\left(1 + e^{-k\lambda}\right)} \tag{9}$$

where

$$\lambda_1 = \frac{\lambda}{a_0 + \lambda} \tag{10}$$

$Y(\lambda_1)$ is a factor which is introduced to account for the stress field in the vicinity of the hole [9]. The dependence of $Y(\lambda_1)$ on λ_1 is shown in Fig. 5. Even in the initial stages of crack growth we assume the cracks to be through thickness in nature rather than semi-circular, on the basis that through-thickness machining marks were presumably present on the interior surfaces of the holes and that these markings promoted the early development of 2D cracks.

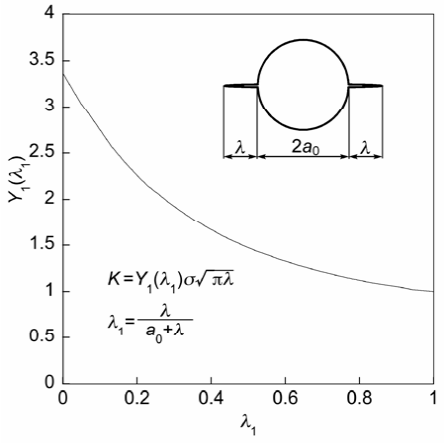

Fig. 5. The dependence of $Y_1(\lambda_1)$ on λ_1.

Fig. 6 compares the results calculations based upon Eq. 4 with the experimental results of El Haddad et al. In Fig. 6, the stress range at the threshold level is shown as function of λ for three hole sizes. This figure also shows the experimentally determined conditions for either crack arrest or crack propagation. A closed symbol indicates the crack length at which a crack was arrested; an open symbol indicates a crack that was not arrested. It is considered that the agreement between our predictions and the experimental results is reasonable.

Fig. 7 is a plot of K_F as function of hole radius. In this plot the results of our analysis are compared with predictions based upon the empirical expressions of Kuhn and Hardrath [5] and Peterson [6]. The predicted fatigue notch sensitivities are in general agreement with these empirical relationships.

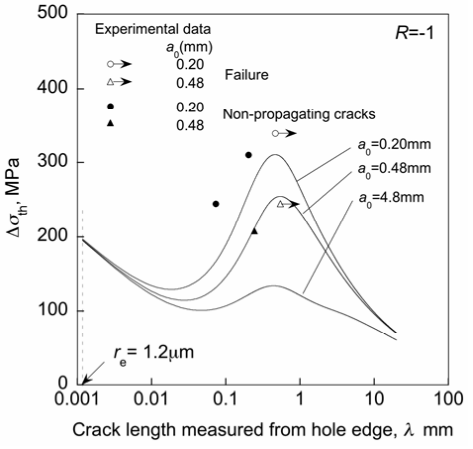

Fig.6. The dependence of $\Delta\sigma_{th}$ on λ for holes of radius 0.20, 0.48 and 4.8 mm.

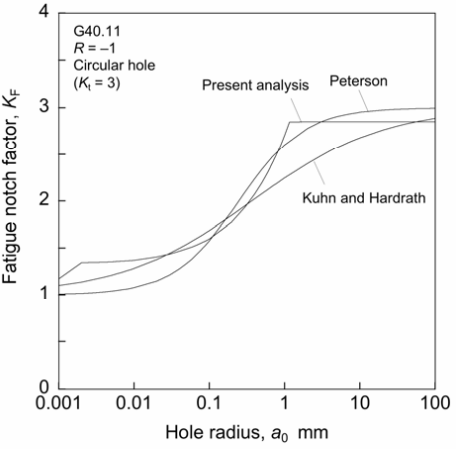

Fig. 7. Dependence of the fatigue notch factor, $K_{F,}$ on size of hole.

VHCF in Ti-6Al-4V

In recent years the relationship between fish-eye, sub-surface fatigue origins and very high cycle fatigue (VHCF) has become a topic of interest, but as of yet there is not a clear understanding of the mechanism which is responsible for the very long fatigue lives. The purpose of the present paper is to present a description of a possible mechanism based upon consideration of the VHCF process in Ti-6Al-4V [10].

Fig. 8 shows the results of axial load fatigue tests carried out at R = 0.1 [11]. It is noted that in the case of subsurface crack initiation the lives range from 10^7 to 10^8 cycles.

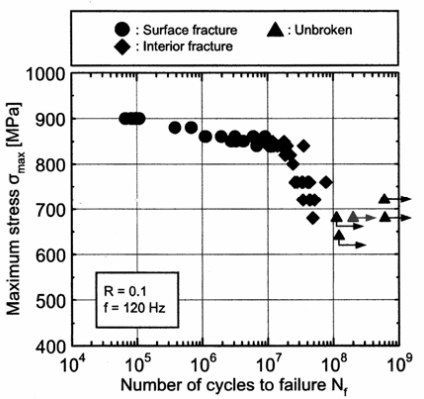

Fig. 8. S/N curve for Ti-6Al-4V [11]

Ishihara [12] has shown that surface fatigue cracks in Ti-6-4 initiate early in life, and we assume that the same holds true for sub-surface crack initiation, particularly because the longest in-air lives are similar to the shortest lives for sub-surface crack initiation. Oguma [13] has noted that for both the surface and subsurface fatigue crack initiation processes in Ti-6-4, 10-micron sized facets, the size of the alpha grains, are formed at the initiation sites. Oguma [13] has also shown that in Ti-6-4

the fracture surface surrounding a sub-surface initiation site is quite rough (stage 2a)(also referred to as the ODA or optically dark area). Stage 2b is characterized by a much smoother fracture surface and may contain striations. Regions 2a and 2b comprise what is referred to as a fish-eye fracture. Fig. 9 shows the fatigue facture surface appearance for the case of surface-initiated fatigue cracking. Fig. 10 shows the fatigue fracture surface appearance in region 2a of sub-surface initiated fatigue cracking. It is seen in Fig. 10 that the sharp fractographic features shown in Fig, 9 have been rounded off.

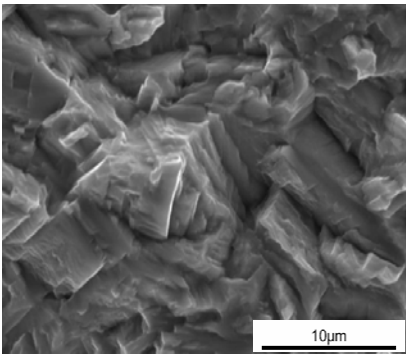

Fig.9. Fatigue fracture surface for case of surface initiated fracture

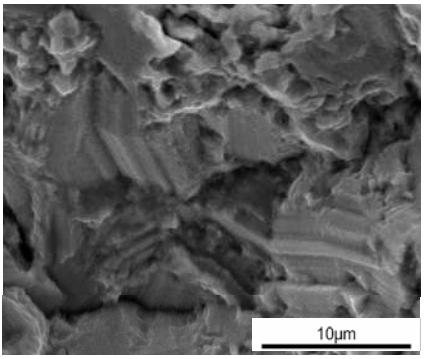

Fig.10. Fatigue fracture surface (stage 2a) for case of sub-surface initiated

In accord with Eq. 4, in order for crack propagation to occur, D, the crack driving force defined as $(\sqrt{2\pi r_e F} + Y\sqrt{\pi a F})\Delta\sigma$, must be greater than R, the crack resisting force defined as $[(1-e^{-ka})(K_{op\max} - K_{\min}) + \Delta K_{effth}]$. Ordinarily, when the driving force is less than the resisting force, crack arrest occurs and a non-propagating crack is formed, as in Fig. 6. We propose that this is the situation in the present case and that it leads to sub-surface crack initiation. Sub-surface VHCF can occur in Ti-6Al-4V (and presumably in other alloys as well) because once a subsurface crack is initiated, the absence of oxygen allows a wear process to take place in Stage 2a which reduces the local crack closure level and thereby enables an otherwise arrested crack to propagate, albeit at a very slow rate. This wear process results in the rounded fractographic features shown in Fig. 10.

Calculations base upon Eq. 4 can be used to describe the driving force and resistance force process more quantitatively. Based upon the data in [13], the following values are deemed to be appropriate for Ti-6Al-4V in vacuum:

Material	σ_Y [MPa]	σ_{uts} [MPa]	$\Delta\sigma_{w0}$ [MPa] $R = 0.1$	k [m^{-1}]	K_{opmax} [$MPam^{-1/2}$]	ΔK_{effth} [$MPam^{-1/2}$]	r_e [μm]
Ti-6Al-4V	899	988	743	50,000	5.0	3.0	0.9

Table 3. Material constants for Ti-6Al-4V

As closure develops with crack advance the resistance to crack growth increases and reaches a maximum at the maximum K_{op} level for the material and the loading pattern.

The effect of the erosion process on the resistance curve is indicated in Fig. 11, and, in a representation similar to Fig 5, in Fig. 12.

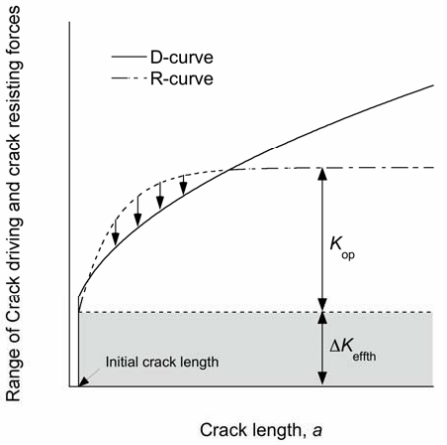

Fig. 11. Schematic example of the reduction by cyclic erosion of the crack resisting force to the level of the crack driving force. The extent of region 2a is indicated [13].

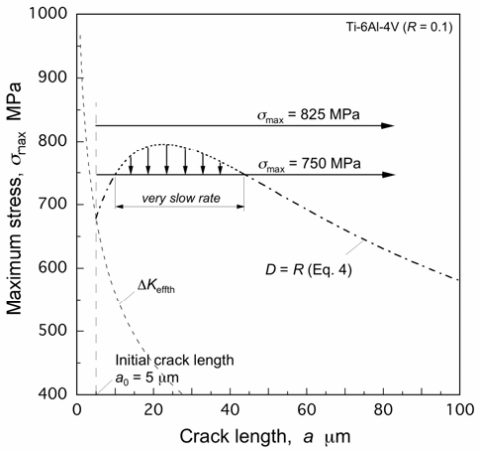

Fig. 12. Effect of erosion on sub-surface crack growth.

The tortuous nature of the stage 2a fracture surface is an indication that the crack front has been probing the material ahead of the front seeking crack paths of minimum resistance to allow the crack to grow. It is this tortuosity that gives rise to much of the roughness-induced crack closure level associated with sub-surface fatigue cracking. Once the crack has reached the outer boundary of the resistance curve, stage 2b is reached and it has been shown [13] that the remaining lifetime is relatively short. It is concluded that the very high cycle fatigue lives observed in subsurface fatigue of Ti-6Al-4V can be accounted for on the basis that crack advance can only occur when the level of crack closure has been reduced by wear to a level allowing the crack to propagate. Most of the lifetime is spent in reducing the crack closure level by the wear process.

Conclusions

1. In the preceding sections it has been shown that short crack growth threshold behavior for initial crack lengths of the order of 10-1000 microns can be successfully analyzed.
2. Further it has been shown that fatigue notch sensitivity can be understood on the basis of short crack growth behavior.
3. Finally the VHCF behavior of Ti-6Al-4V can be understood based upon the concepts introduced herein and the need for crack closure levels to be reduced by a process of wear.

References

[1] A. J. McEvily: Mater. Sci. Forum Vol. 482 (2005), p. 3-10

[2] A. J. McEvily, S. Ishihara, M. Endo, H. Sakai and H. Matsunaga: Int. J. Fatigue Vol. 29-12 (2007), p. 2237-2245

[3] A. J. McEvily, B. Bryce, and R. O. Ritchie, unpublished research.

[4] Y. Kondo, C. Sakae, M. Kubota, and M. Kashiwagi: J. ASTM Int Vol. 2 (2005) paper ID JAI11990 (information on www.astm.org)

[5] P. Kuhn and H. F. Hardrath, in: An engineering method for estimating the notch-size effect in steels. NACA TN 2805 (1952)

[6] R. E. Peterson, in: Stress concentration factors. New York, John Wiley (1974)

[7] Design handbook of fatigue strength of metals. Tokyo: Japan Society of Mechanical Engineers (JSME) Vol. 1 (1982), p. 125

[8] M. H. El Haddad, T. H. Topper, K. N. Smith: Eng Fract Mech Vol. 11 (1979), p.573-584

[9] Y. Murakami et al. in: Stress intensity factors handbook. Oxford: Pergamon Press (1987)

[10] A. J. McEvily, T. Nakamura, H. Oguma, M. Endo and H. Mtsunaga: submitted for publication

[11] T. Nakamura, H. Oguma and T. Shiina, in press.

[12] K. Komano, S. Ishihara, A. J. McEvily and H. Shibata: 2007, available on line from Trans Tech Publications, Switzerland.

[13] H. Oguma, PhD Thesis, Hokkaido Univ., 2006.